Remote Sensing of Environment 204 (2018) 138–146

Contents lists available at ScienceDirect

Remote Sensing of Environment

journal homepage: www.elsevier.com/locate/rse

Modeling re-absorption of fluorescence from the leaf to the canopy level

Juan M. Romero[a,b], Gabriela B. Cordon[c,d], M. Gabriela Lagorio[a,b,*]

[a] Universidad de Buenos Aires, Facultad de Ciencias Exactas y Naturales, Departamento de Química Inorgánica, Analítica y Química Física, Buenos Aires, Argentina
[b] CONICET - Universidad de Buenos Aires, Instituto de Química Física de los Materiales, Medio Ambiente y Energía (INQUIMAE), Buenos Aires, Argentina
[c] Universidad de Buenos Aires, Facultad de Agronomía, Área de Educación Agropecuaria, Buenos Aires, Argentina
[d] CONICET - Universidad de Buenos Aires, Instituto de Investigaciones Fisiológicas y Ecológicas Vinculadas a la Agricultura (IFEVA), Buenos Aires, Argentina

ARTICLE INFO

Keywords:
Chlorophyll fluorescence
Canopy
Light re-absorption
Remote sensing
Photophysical modeling

ABSTRACT

Chlorophyll fluorescence is widely used as an indicator of photosynthesis and physiological state of plants. Remote acquisition of fluorescence allows the diagnosis of large field extensions, even from satellite measurements. Nevertheless, fluorescence emerging from chloroplasts, the one directly connected to plant physiology, undergoes re-absorption processes both within the leaf and the canopy. Therefore, corrections of the observed canopy fluorescence, taking into account these two re-absorption processes may help to draw accurate inferences about plant health. Here, we show the theoretical development and experimental validation of a model that allows to retrieve the spectral distribution of the leaf fluorescence spectrum from that on top of canopy (TOC) using a correction factor which is a function of both canopy and soil reflectance, and canopy transmittance. Canopy fluorescence spectra corrected by our theoretical approach and normalized shows 95% correlation with the normalized fluorescence spectrum at leaf-level, thus validating the model. Therefore, our results provide a physical explanation and quantification for fluorescence re-absorption within the canopy, a phenomenon which has only been mentioned but never measured up to the date. From a more general perspective, this new analytical tool together with the one previously developed by Ramos and Lagorio (2004) allows to obtain the spectral distribution of chloroplast fluorescence spectrum from that on top of canopy (TOC).

1. Introduction

In photosynthetic organisms, chlorophyll-a excited states, produced either by direct absorption or by energy transfer, can decay by three main pathways: electron transfer (which initiates photosynthesis), heat dissipation and light emission as fluorescence. These three processes are competitive with each other and, in consequence, an increase in the efficiency of one of them leads to a decrease in the efficiency of one or both of the other two. This competition is the key for the existing link between photosynthesis and chlorophyll fluorescence (Maxwell and Johnson, 2000).

Thus, analysis of chlorophyll fluorescence from vegetation can give information on photosynthesis and on the physiological state of plants (Maxwell and Johnson, 2000; Moya and Cerovic, 2004; Guanter et al., 2014). This largely contributes to a better understanding of environmental and anthropogenic effects on vegetation physiology and also on carbon fluxes between plants and the atmosphere, thus providing the key for the assessment of greenhouse effect and, ultimately, global warming (Grace et al., 2007). Chlorophyll fluorescence may be studied from different observation scales: ground, airborne and spaceborne. An excellent review of the methods and equipment used in each case is presented by Meroni et al. (2009).

For the remote sensing of chlorophyll fluorescence from vegetation, passive and active methods have been developed. While passive methods use polychromatic sunlight excitation (Louis et al., 2005; Meroni and Colombo, 2006; Guanter et al., 2007), active procedures use a high energy LASER as irradiation source with LiDAR (Laser imaging detection and ranging system) technology from an airborne (Cerovic et al., 1996; Ounis et al., 2016).

The interaction of light with canopies is a subject of great interest in the remote monitoring of plant health and it was described in literature by means of radiative transfer models (RTM) which are often used to describe the propagation of photons through a medium where they are affected by absorption, emission and scattering processes. Computational methods are required to solve the mathematical equations involved in these models. In particular, for remote sensing of vegetation, several RTM have been developed: PROSPECT simulates reflectance and transmittance of leaves, from 400 nm to 2500 nm (Jacquemoud and Baret, 1990); LIBERTY (*Leaf Incorporating Biochemistry Exhibiting Reflectance and Transmittance Yields*) calculates the

* Corresponding author at: Universidad de Buenos Aires, Facultad de Ciencias Exactas y Naturales, Departamento de Química Inorgánica, Analítica y Química Física, Buenos Aires, Argentina.
E-mail address: mgl@qi.fcen.uba.ar (M.G. Lagorio).

http://dx.doi.org/10.1016/j.rse.2017.10.035
Received 22 April 2017; Received in revised form 6 October 2017; Accepted 21 October 2017
Available online 07 November 2017
0034-4257/

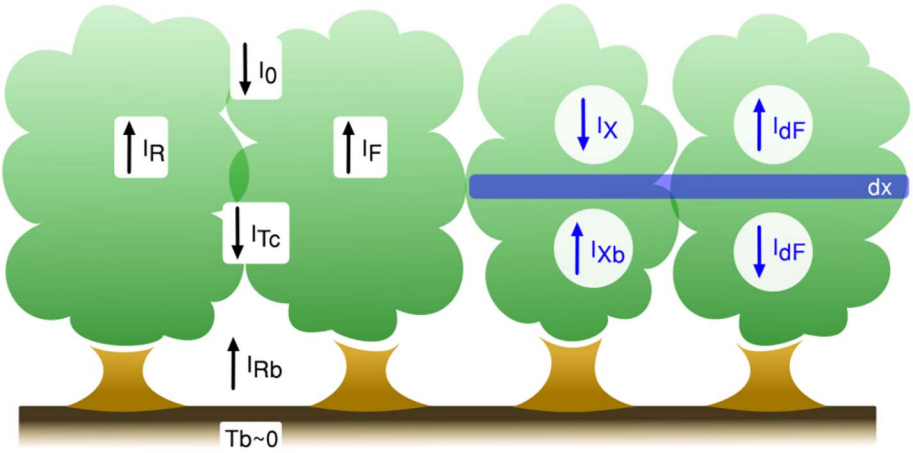

Fig. 1. Canopy model. Photon fluxes involved in the interaction between light and canopy, as assumed by our model. Light attenuation within the canopy was described by a mono-exponential decay in all the cases.

optical properties of conifer needles (Dawson et al., 1998); DLM (dorsiventral leaf radiative transfer model) (Stuckens et al., 2009) is a PROSPECT-like leaf optical model which includes leaves asymmetry; DART (Gastellu-Etchegorry et al., 2012) is a model for remote sensing images and radiative budget and FLIGHT simulates the observed reflectance response of three-dimensional vegetation canopies (North, 1996). Some RTM include fluorescence simulations such as the FluorMODleaf (Pedrós et al., 2010), the Fluspect-B (Vilfan et al., 2016) and FluorWPS (Zhao et al., 2016) models, which predict fluorescence spectra.

Different precision levels (from 1 to 3 dimensions) of canopy description may be found in the RTM. 1D models are the simplest approaches assuming a horizontal layer of vegetation and they are appropriate for homogeneous canopies. 3D models include canopy heterogeneity and they are more realistic (North, 1996; Gastellu-Etchegorry et al., 2012). However, to take into account canopy heterogeneity, 3D models require larger amounts of field data compared to 1D models (Ligot et al., 2014).

Chlorophyll fluorescence from plants is characterized by two peaks at about 685 and 735 nm (Mazzinghi et al., 1994). The red emission peak is due to the radiative deactivation of excited photosystem II (PSII) while the far-red emission one has contributions of both photosystems (PSI and PSII) (Agati, 1998; Pfündel, 1998; Franck et al., 2002; Iriel et al., 2014). The quotient between the red and far-red maxima fluorescence is usually referred to as fluorescence ratio and largely used as an indicator of the plant physiological state (Wittenberghe et al., 2014; Rossini et al., 2016). This ratio was connected with the underlying mechanism of photosynthesis and was reported as an instant monitor of CO_2 uptake by plants (Freedman et al., 2002; Rascher et al., 2009; Damm et al., 2010). Moreover, fluorescence emerging from chloroplasts suffers re-absorption processes in the leaf (Agati et al., 1993; Gitelson et al., 1998; Ramos and Lagorio, 2004; Cordon and Lagorio, 2006). In turn, fluorescence photons emerging from the leaves undergo additional re-absorption in the canopy (Porcar-Castell et al., 2014). As a result, the spectral distribution of fluorescence observed by a remote sensor is completely distorted by this phenomenon. An important point in the analysis of chlorophyll fluorescence is that it is actually the fluorescence of the chloroplasts (and not the "observed" fluorescence from a canopy) which is directly connected to the physiological state of the plant. Several groups have previously developed and applied models to perform corrections for light re-absorption processes in leaves (Agati et al., 1993; Ramos and Lagorio, 2004; Cordon and Lagorio, 2006) but, until now, there are no available models that shed light on these complex processes occurring in canopies.

Rossini et al., 2016 already modeled the fluorescence ratio for different canopies. These authors observed that the ratio between red and far-red fluorescence peaks was considerably lower at canopy level than the one measured on single leaves, attributing this fact to the re-absorption of the red component within the canopy layers. Julitta et al. (2016) recently published a detailed analysis of the red/far-red fluorescence ratio remotely measured by different spectroradiometers. They compared each result with the leaf level value to detect which spectrometer provided the most accurate quantity. They made it clear, however, that the observed fluorescence ratio for the canopy should be lower than the observed fluorescence ratio at leaf level, as the red emission was more affected by re-absorption in the canopy than the far-red band. Fournier et al. (2012) compared the fluorescence emission of a natural grass canopy with the leaf level fluorescence spectrum and they found that the red-to-far-red fluorescence ratio decreased from the leaf to the canopy level. They attributed this effect to a preferential re-absorption of the red fluorescence band but no quantitative estimation of this effect was performed. Another recent work reporting fluorescence re-absorption in a canopy was published by Daumard et al. (2012) who performed passive fluorescence measurements at 687 and 760 nm on sorghum. They effectively observed a decrease in the fluorescence ratio red/far-red for the canopy compared to the leaf-level. Again, preferential light re-absorption in the red was correctly argued but a quantitative support was lacking.

Therefore, although the re-absorption of light within a canopy was profusely cited or qualitatively described in many works, it was never quantitatively corrected. The goal of this work was to present a method to correct active fluorescence measurements by the processes of light absorption that take place in the canopy, filling an important vacancy in the literature. More precisely, the scope of the present study was the development and validation of a model that corrected fluorescence re-absorption within a canopy and that allowed to retrieve the fluorescence spectral distribution at leaf level. Moreover, in combination with other pre-existing approaches, it allowed to recover the fluorescence spectral distribution of the chloroplast from that of the plant cover.

2. Model description and deduction

A pictorial description of the canopy physical model is presented in Fig.1. The physical approach developed in this work considered the following assumptions:

i) the system is composed by the canopy and the soil, ii) no light is transmitted through the whole system (canopy + soil), iii) the light suffers mono-exponential attenuation within the canopy, iv) the plant canopy is composed by fluorescent units (leaves), v) the fluorescence emitted by leaves is reabsorbed in the canopy before leaving it, vi) the re-absorption process also produces a mono-exponential attenuation of fluorescence within the canopy, vii) fluorescence is emitted isotropically within the canopy, viii) lateral light losses are neglected, ix) light scattering is taken into account by considering an effective path length.

The model described here is based on mathematical treatments

previously described in literature for other systems (Agati et al., 1993; Ramos and Lagorio, 2006).

Our starting model is based on a homogeneous vegetation cover which is reached by sunlight and that grows on a thick layer of soil. The assembly canopy + soil does not transmit light. Consequently, the incident photons reaching the canopy (I_0) are partly reflected (I_R) and partly absorbed (I_a) by the system (Eq. (1)). The absorbed light has strictly two contributions: the photon flux absorbed by the canopy (I_{ac}) and the photon flux absorbed by the soil or background (I_{ab}) (Eq. (2)).

$$I_0 = I_R + I_a \tag{1}$$

$$I_a = I_{ac} + I_{ab} \tag{2}$$

The photon flux absorbed by the soil may in turn be estimated by Eq. (3).

$$I_{ab} = I_{Tc}(1 - R_b), \tag{3}$$

where I_{Tc} is the photon flux transmitted by the canopy and R_b is the background reflectance. The factor (1-R_b) represents the fraction of light absorbed by the soil.

Substituting Eqs. (2) and (3) into Eq. (1) and dividing by I_0, Eq. (4) arises:

$$1 = R + a_c + T_c(1 - R_b), \tag{4}$$

where R is the total reflectance of the system, a_c is the fraction of light absorbed by the canopy and T_c is the canopy transmittance. The fraction of light not absorbed by the canopy may then be written as:

$$1 - a_c = R + T_c(1 - R_b). \tag{5}$$

Let us consider a thin differential layer of canopy dx (Fig. 1) receiving a photon flux $I_x(\lambda)$ which comes from the attenuation of the incident beam I_0. This attenuation is supposed to be exponential and is described by Eq. (6).

$$I_x(\lambda_0) = I_0(\lambda_0)\cdot\exp[-\alpha(\lambda_0)\cdot x(\lambda_0)], \tag{6}$$

where λ_0 is the excitation wavelength, $\alpha(\lambda)$ is the absorption coefficient of the canopy and $x(\lambda_0)$ is an effective pathlength at the excitation wavelength that is affected by the presence of light scattering.

The infinitesimal layer also receives light from below which results from the attenuation of a back photon flow in the canopy (Fig. 1).

$$I_{xb}(\lambda_0) = I_b(\lambda_0)\cdot\exp[-\alpha(\lambda_0)\cdot x_b(\lambda_0)], \tag{7}$$

where the absorption coefficient of the canopy $\alpha(\lambda)$ was assumed equal for both descending and ascending photon fluxes.

Traversing the infinitesimal layer both beams suffer additional exponential attenuation: $I_x(\lambda_0)\exp[-\alpha(\lambda_0)\cdot dx]$ and $I_{xb}(\lambda_0)\exp[-\alpha(\lambda_0)\cdot dx]$ respectively. Since the number of photons absorbed by the layer can be calculated as the number that enters the layer minus the number coming out, we can write Eq. (8) for the photon flux absorbed by the layer:

$$\begin{aligned} &I_x(\lambda_0) + I_{xb}(\lambda_0) - \{I_x(\lambda_0)\cdot\exp[-\alpha(\lambda_0)\cdot dx] + I_{xb}(\lambda_0)\cdot\exp[-\alpha(\lambda_0)\cdot dx]\} \\ &= I_x(\lambda_0)\{1 - \exp[-\alpha(\lambda_0)\cdot dx]\} + I_{xb}\{1 - \exp[-\alpha(\lambda_0)\cdot dx]\}. \end{aligned} \tag{8}$$

Taking into account that the spectral distribution of photons generated as fluorescence may be calculated as the fluorescence quantum yield of the system (ϕ_F) multiplied by the spectral distribution of fluorescence $g(\lambda)$ (normalized to unity area, i.e.: $\int_\lambda g(\lambda)d\lambda = 1$) and by the absorbed photon flux, the fluorescence photon flow originated in the infinitesimal layer, which is emitted isotropically within the canopy, may be calculated by Eq. (9).

$$\begin{aligned} dI_F(\lambda) = \phi_F\cdot g(\lambda)\ &[I_x(\lambda_0)\{1 - \exp[-\alpha(\lambda_0)dx]\} \\ &+ I_{xb}(\lambda_0)\{1 - \exp[-\alpha(\lambda_0)dx]\}]. \end{aligned} \tag{9}$$

Eq. (9) may be then approximated to Eq. (10) taking into account the mathematical rule that when $w \to 0$, $1 - \exp(w) \sim -w$ and substituting I_x and I_{xb} by Eqs. (6) and (7). Notice that, as dx is an infinitesimal quantity, the linear approximation to the exponential function $\exp[-\alpha(\lambda_0)dx]$ may be assumed valid for any $\alpha(\lambda_0)$ value.

$$\begin{aligned} dI_F(\lambda) = \phi_F\cdot g(\lambda)\cdot[I_x(\lambda_0)\alpha(\lambda_0)dx + I_{xb}(\lambda_0)\alpha(\lambda_0)dx] = \phi_F\cdot g(\lambda)\cdot\alpha(\lambda_0) \\ \cdot\exp[-\alpha(\lambda_0)\cdot x(\lambda_0)]\cdot[I_0(\lambda_0) + I_b(\lambda_0)]\cdot dx \end{aligned} \tag{10}$$

Now, to introduce the re-absorption processes affecting the fluorescence, we assume that this phenomenon produces an exponential attenuation of $dI_F(\lambda)$ and that the fluorescence reaching the top of canopy travels an average effective pathlength $x(\lambda)$ (Eq. (11)),

$$\begin{aligned} dI_F(\lambda)^{exp} = \phi_F\cdot g(\lambda)\cdot\alpha(\lambda_0)\cdot\exp[-\alpha(\lambda_0)\cdot x(\lambda_0)]\cdot[I_0(\lambda_0) + I_b(\lambda_0)] \\ \cdot\exp[-\alpha(\lambda)\cdot x(\lambda)]dx \end{aligned} \tag{11}$$

where $dI_F(\lambda)^{exp}$ is the photon flux generated in the thin layer affected by light re-absorption and $x(\lambda)$ is the effective optical pathlength that takes into account the light scattering in the media and it may be expressed as.

$$x(\lambda) = x(\lambda_0)\cdot f(\lambda), \tag{12}$$

where the function $f(\lambda)$ reflects the wavelength dependence of the scattering coefficient.

Replacement of Eq. (12) into Eq. (11) and integration of both Eqs. (10) and (11), between x = 0 and the maximum mean effective optical pathlength = $X(\lambda_0)$, leads to Eqs. (13) and (14) respectively:

$$I_F(\lambda) = I_F{}^{corr}(\lambda) = \phi_F g(\lambda)[I_0(\lambda_0) + I_b(\lambda_0)]\{1 - \exp[-\alpha(\lambda_0)\cdot X(\lambda_0)]\}. \tag{13}$$

$I_F(\lambda)$ represents the fluorescence intensity free from light re-absorption processes and is renamed as corrected fluorescence intensity $I_F(\lambda)^{corr}$ to consider this feature.

$$\begin{aligned} I_F(\lambda)^{exp} = \phi_F g(\lambda)[I_0(\lambda_0) + I_b(\lambda_0)]\{1 - \exp[-\alpha(\lambda_0) + \alpha(\lambda)\cdot f(\lambda) \\ \cdot X(\lambda_0)]\}\frac{\alpha(\lambda_0)}{\alpha(\lambda_0) + \alpha(\lambda)f(\lambda)} \end{aligned} \tag{14}$$

As Eq. (13) derives from Eq. (10), where no light re-absorption is considered, and Eq. (14) comes from Eq. (11) that includes re-absorption, the ratio between both equations (Eq. (15)) gives the correction factor for this process.

$$\begin{aligned} I_F(\lambda)^{corr}/I_F(\lambda)^{exp} &= \frac{\{1 - \exp[-\alpha(\lambda_0)\cdot X(\lambda_0)]\}\cdot[\alpha(\lambda_0) + \alpha(\lambda)f(\lambda)]}{\{1 - \exp[-\alpha(\lambda_0) + \alpha(\lambda)f(\lambda)X(\lambda_0)]\}\cdot\alpha(\lambda_0)} \\ &= \chi(\lambda, \lambda_0), \end{aligned} \tag{15}$$

where $\chi(\lambda, \lambda_0)$ represents the correction factor that takes into account light re-absorption processes within the canopy.

In fact, the product between the experimental fluorescence spectrum and the correction factor yields the fluorescence spectrum free from re-absorption distortion.

Following Eq. (12), the product $f(\lambda)X(\lambda_0)$ in Eq. (15) is equal to $X(\lambda)$ which represents the effective average pathlength at different wavelengths. Consequently, the product between the absorption coefficient and the effective average pathlength $\alpha(\lambda)\cdot X(\lambda)$ may be considered as the effective absorption spectrum of the canopy, and the fraction of light non-absorbed by the canopy ($\xi(\lambda)$) may be estimated as:

$$\xi(\lambda) = \exp[-\alpha(\lambda)\cdot X(\lambda)] \tag{16}$$

From Eqs. (15) and (16), an expression of the correction factor as a function of the fraction of non-absorbed light by the canopy may be written (Eq. (17)):

$$\chi(\lambda, \lambda_0) = \left[1 + \frac{\ln\xi(\lambda)}{\ln\xi(\lambda_0)}\right]\cdot\left[\frac{1 - \xi(\lambda_0)}{1 - \xi(\lambda_0)\xi(\lambda)}\right]. \tag{17}$$

As $\xi(\lambda)$ may be estimated as $R + T_c(1 - R_b)$ (see Eq. (5)), $\chi(\lambda,\lambda_0)$ may be easily estimated from measures available experimentally.

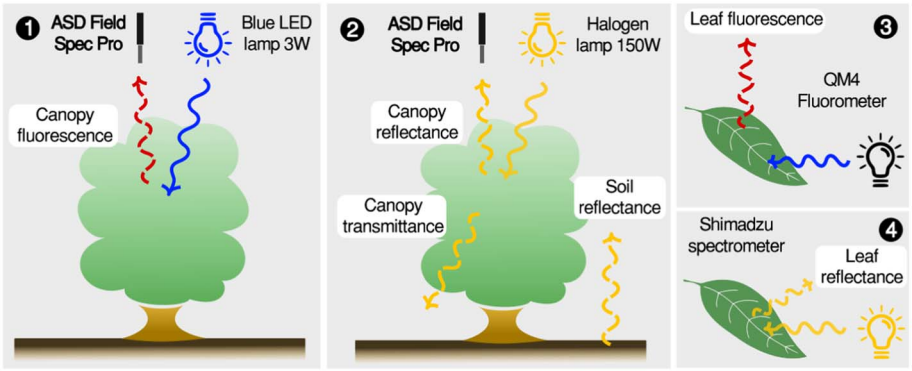

Fig. 2. Chart displaying the performed measurements.

3. Materials and methods

3.1. Canopy-level measurements

Radiance, reflectance and transmittance spectra of plants were performed by means of a spectroradiometer ASD FieldSpec Pro FR (Analytical Spectral Devices Inc., Boulder, USA), using a sensor field of view (FOV) of 23° (Fig. 2). The spectral range of this equipment varied between 350 nm to 2500 nm and its spectral resolution was 3 nm in the range 350–1000 nm with a sampling interval of 1.4 nm. In the zone between 1000 and 2500 nm of the electromagnetic spectrum, the spectral resolution was 10 nm with 2 nm of sampling interval.

To record the canopy emission, fluorescence emitted by a *Ficus benjamina* plant was recorded when excited by a 3 W blue LED lamp (λ_{max} = 460 nm, see emission spectrum in Fig. 4) with a photon flux of 50 ± 10 μmol/m^2 s. In all the cases, photon fluxes were measured by a photodiode connected to a multimeter (SR45–Fieldmaster, Coherent Inc., Santa Clara, CA 95054 USA). The *F. benjamina* plant was placed in a matte black wooden box (60 cm × 60 cm × 120 cm) with the lamp and with an optic fiber inside, which was connected to the ASD spectroradiometer. In the upper part of the box, a small opening was made through where the wires of the blue LED lamp and the optic bare fiber of the spectroradiometer ASD were introduced. The distance between the tip of the optic fiber and the upper leaves of the plant was 50 cm, which led to a sampling area of 22 cm diameter approximately.

With the box closed, several measures were made. At first, white reference spectra were collected by recording the light reflected by a Spectralon® panel (Labsphere Inc., North Sutton, USA). The fluorescence spectra (between 600 and 800 nm) induced in plants by the blue light were computed from the plant radiance. Collection was done with the plant in ten different positions and ten spectra were acquired each time. As the radiance was recorded with the ASD spectroradiometer, the units for the fluorescence spectra were W m^{-2} nm^{-1} sr^{-1}. These units were converted into number of photons (counts) for the subsequent comparison with the fluorescence spectra recorded by standard fluorometry. Kautsky effect was evaluated in order to make it sure to measure fluorescence spectra in steady state. Plants were dark-adapted for 15 min, and then the blue LED lamp was turned on. Radiance spectra were then immediately recorded every 10 s until constant shape in the fluorescence spectral distribution (see Fig. 3).

Total reflectance and canopy transmittance as well as background reflectance were obtained by irradiating with a halogen lamp (Philips lamp Spotone 150 W, 230 V). Reflectance spectra, i.e. the proportion of the incident radiation that is reflected by plant surface at each wavelength, were calculated as the ratio between plant radiance and the incident light which was determined by means of the Spectralon® panel. As it was done with fluorescence, ten spectra in ten different plant positions were recorded. To obtain transmittance spectra, the optical fiber was placed under the plant in different positions and radiance was registered each time. Then, transmittance spectra were calculated by performing the ratio between this radiance and the incident light. For the background reflectance the radiance from the soil was divided by the incident light flux. Canopy transmittance and background reflectance were registered ten times in a unique plant position, due to its low variance.

3.2. Leaf-level measurements

In order to obtain leaf fluorescence spectra, 15 plant leaves were cut right after measuring radiance in the box and their spectra were immediately obtained. Measurements were performed on the adaxial face using groups of six leaves to avoid transmission of light through them. Leaf fluorescence spectra were recorded with a steady-state fluorometer QM4-CW (Photon Technology Inc., London, Ontario, Canada) in the spectral region between 600 and 800 nm and corrected by the detector response to different wavelengths. Excitation wavelength was 460 nm, the excitation slit width was set to 8 nm, the emission slit width was adjusted enough to record an adequate signal (2 nm) (Fig. 2). Under these conditions, photon flux was 60 ± 10 μmol/m^2 s, similar to the photon flux used in the measurements made in the box. Care was taken to assure that leaf and canopy spectra were measured in steady state (Lichtenthaler et al., 2005), as variable fluorescence (Kautsky effect) was observed upon turning on the blue light (see Fig. 3).

Reflectance spectra of leaves were recorded by means of a Shimadzu 3101 spectrophotometer equipped with an integrating sphere. Barium sulfate was used as a standard to adjust the 100% reflectance level. Again, measurements were performed on the adaxial face using groups of six leaves to avoid transmission of light through them (a necessary condition to apply the model that corrects light re-absorption artifacts at leaf level) (Ramos and Lagorio, 2004; Cordon and Lagorio, 2006).

3.3. Data analysis

Spectra were processed using Python programming language (Zelle, 2004) together with NumPy numerical package (van der Walt et al., 2011). Statistical analysis was conducted by the Infostat software (Di Rienzo et al., 2011). Figures were designed and created by the Inkscape program (Bah, 2009). Canopy fluorescence spectra were corrected by Eq. (15), taking into account Eqs. (17) and (5). Resulting fluorescence spectra were additionally corrected according to Ramos and Lagorio (2004), in order to obtain the fluorescence spectra of chloroplasts.

4. Model validation

The model was validated by comparing corrected canopy fluorescence spectra with leaf fluorescence spectra. The validation process required the experimental collection of canopy fluorescence spectra which, to our knowledge, had never been recorded before. In fact, most of the works reporting remote detection of chlorophyll fluorescence involve the Fraunhofer and telluric line discrimination methodology

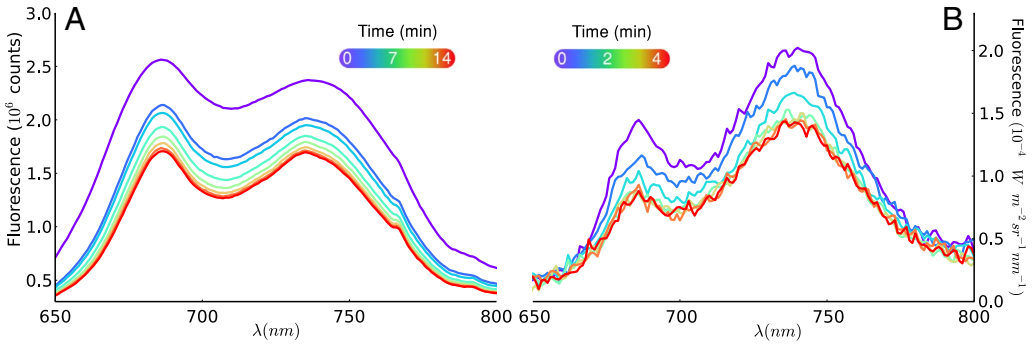

Fig. 3. Kaustky effect. Variable fluorescence effect observed upon blue light illumination after 15 min dark adaptation; both at leaf (A) and canopy level (B). Time intervals are shown using a colour scale. Note the different timescales and fluorescence units at each level. (For interpretation of the references to colour in this figure legend, the reader is referred to the web version of this article.)

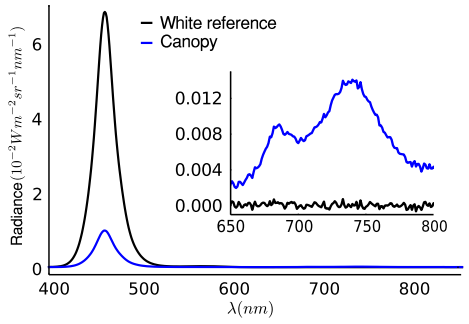

Fig. 4. Canopy fluorescence spectrum. Example of the radiance registered by the ASD spectrometer while measuring in the box. Incident light radiance obtained from the white 100% reflectance standard (black line) showing a single peak at λ = 460 nm. Plant radiance (blue line) displaying reflection of incident light and chlorophyll fluorescence spectrum between 650 and 800 nm (inset). Note that the inset arises from an enlargement of the scales of the axes. (For interpretation of the references to colour in this figure legend, the reader is referred to the web version of this article.)

which only allows obtaining one or two points of the spectrum (Joiner et al., 2012; Porcar-Castell et al., 2014). Fig. 4 shows an example of the experimental canopy spectrum obtained from the radiance of the plant measured by a spectroradiometer calibrated with a white reflectance standard. Even though the fluorescence spectrum is obtained with some noise due to its low intensity, it is reasonably retrieved from the radiance measurements.

Upon measuring the required parameters for the calculation of the factor $\chi(\lambda,\lambda_0)$, the corrected canopy spectrum was obtained (see Fig. 5). As seen in Fig. 6A, a very good agreement was found between the normalized corrected canopy spectrum and the normalized experimental fluorescence spectrum at leaf level. Moreover, the correlation between the leaf level and the corrected canopy fluorescence values is shown in Fig. 6B, where the slopes of the obtained and expected relationships differ less than 5%. We compare normalized spectra because it is not expected to have an agreement between leaf spectrum and the corrected canopy spectrum in physical units (absolute intensities), given that the absolute values depend on the canopy biomass. Once the distortion by light re-absorption processes is eliminated, the spectral shape (or distribution) is expected to show agreement in both cases. Regarding the red/far-red peak ratios, they are also corrected by the proposed model, leading to the following values: leaf = 0.98 ± 0.14 (n = 15), canopy = 0.60 ± 0.08 (n = 10) and corrected canopy = 0.91 ± 0.13 (n = 10). Even though the model presented here was validated on *Ficus benjamina* plants, further work on extending its validity to other species, different canopy structures, and degrees of heterogeneity would be fruitful.

5. Influence of different factors

Furthermore, we have analyzed the influence of the different factors affecting light re-absorption correction. To achieve this, the

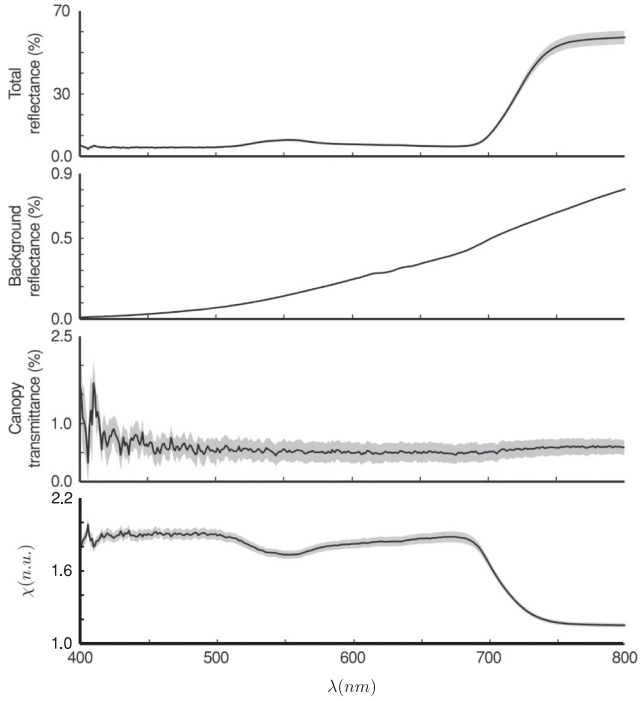

Fig. 5. Measured and calculated parameters. Black lines represent the average value and grey shadows the standard error (n = 10). Note the different scales in each graph.

experimental spectra for total reflectance, background reflectance and canopy transmittance were multiplied by a factor (F) varying from 0 to 10. Values for F leading to spectra with no physical meaning (reflectance or transmittance higher than 1) were not considered. The $\chi(\lambda,\lambda_0)$ function was then obtained by using the spectra calculated with each F value and plotted as a function of wavelength. In Fig. 7B and C it may be observed that the canopy correction factor $\chi(\lambda,\lambda_0)$ was not affected appreciably by the effect of altering the reflectance of the background or the canopy transmittance. On the other hand, the correction factor is very sensitive to variations in the total reflectance (Fig. 7A). In fact, as the total reflectance increased (blue to green colours for curves) $\chi(\lambda,\lambda_0)$ value decreases. The higher the $\chi(\lambda,\lambda_0)$ value, the greater the importance of re-absorption. In Fig. 7 it is shown that light re-absorption is more significant in the red than in the far-red region as expected. A value equal to 1 for $\chi(\lambda,\lambda_0)$ would represent a hypothetical case where no light re-absorption is taking place. Accordingly, $\chi(\lambda,\lambda_0)$ values are closer to 1 in the far-red region, where light re-absorption processes are almost negligible.

6. From canopy to chloroplasts

As it is possible to retrieve the fluorescence spectra of chloroplasts from those at leaf-level by measuring leaf reflectance (Ramos and

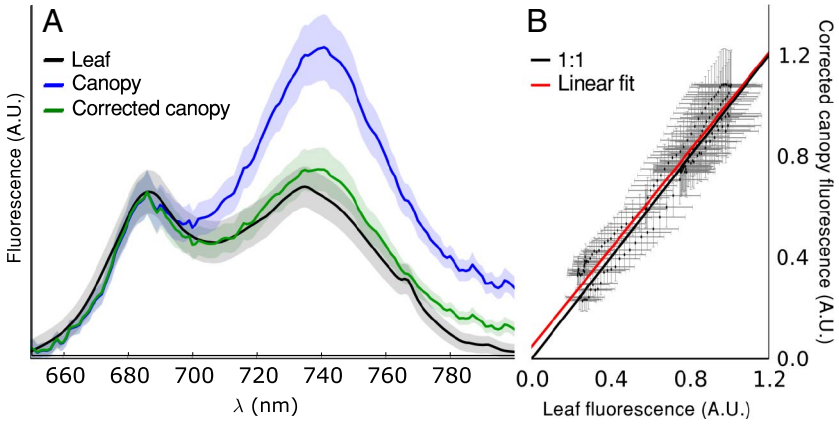

Fig. 6. Model validation. (A) Leaf, canopy and corrected canopy fluorescence spectra are shown in black, blue and green, respectively. Spectra are normalized at the red peak (λ = 686 nm). Shadows indicate the standard error. (B) Correlation between the canopy fluorescence data corrected by light re-absorption (average, n = 10) and leaf fluorescence data (average, n = 15). Red line stands for the best linear fit (y = (0.97 ± 0.02) ∗ x + (0.05 ± 0.01), R^2 = 0.94) and black line represents the 1:1 curve. Each spectrum was normalized at λ = 686 nm. (For interpretation of the references to colour in this figure legend, the reader is referred to the web version of this article.)

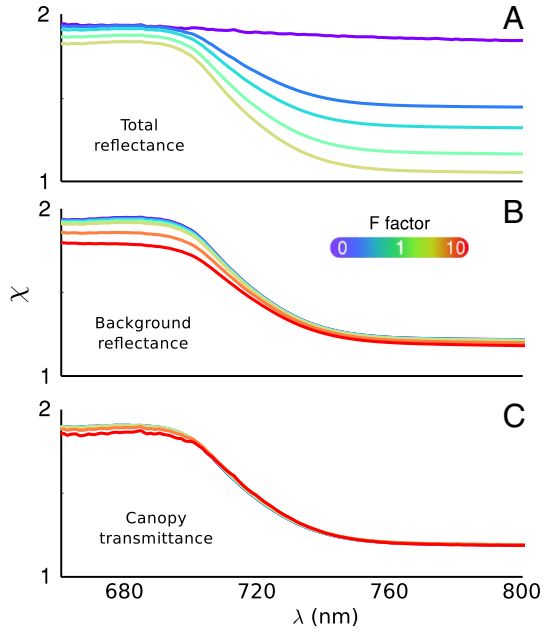

Fig. 7. Influence of different factors on the re-absorption correction for canopy fluorescence. Influence of total reflectance spectra (A), background reflectance (B) and canopy transmittance (C) on the correction factor χ. Each original spectrum is multiplied by a factor F ranging from 0 to 10 (shown in logarithmic colour scale).
Note: For A there are not red curves in the plot because F values close to 10 led to total reflectance values higher than 1, which do not have physical meaning.

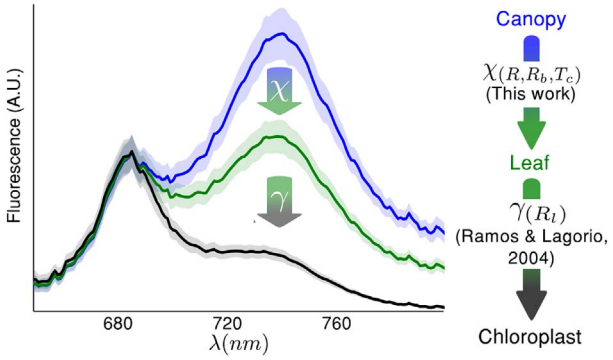

Fig. 8. Chlorophyll fluorescence spectra, from canopy to chloroplasts. Experimental canopy fluorescence spectrum (blue line), retrieved fluorescence spectrum at leaf level using the model presented in this work (green line) and retrieved fluorescence spectrum at chloroplast level from the corrected canopy spectrum using the model described by Ramos and Lagorio (2004) (black line). In this figure R, R_b, T_c and R_l stand for total reflectance, background reflectance, canopy transmittance and leaf reflectance (stacked of six leaves) respectively (n = 10). (For interpretation of the references to colour in this figure legend, the reader is referred to the web version of this article.)

Lagorio, 2004), we were able to predict the chloroplast spectrum starting from that of the canopy (Fig. 8).

The fluorescence ratio (red/far-red) observed at the TOC may also be corrected by the χ(λ) factor developed in this work and by γ(λ), applied for the first time to leaves by Ramos and Lagorio (2004). In fact, by dividing the spectral distribution of leaf fluorescence by the function γ(λ), the spectral distribution of fluorescence for a chloroplast is retrieved. This correction function is calculated by Eq. (18)

$$\gamma(\lambda,\lambda_0) = \frac{1}{1+\sqrt{\frac{F(R_\lambda)}{F(R_\lambda)+2}}} \cdot \frac{1}{1+\sqrt{\frac{F(R_\lambda)\cdot(F(R_\lambda)+2)}{F(R_{\lambda_0})\cdot(F(R_{\lambda_0})+2)}}}. \quad (18)$$

The function γ(λ) depends both on the excitation (λ_0) and emission (λ) wavelength and is obtained from the remission function $F(R_\lambda)$ (Eq. (19)) which is calculated from the reflectance of an opaque sample (Transmittance = 0) as:

$$F(R_\lambda) = \frac{(1-R_\lambda)^2}{2R_\lambda}. \quad (19)$$

The function γ(λ) is derived from a two flux model based on the Kubelka-Munk theory of diffuse reflectance (Lagorio et al., 1998). In this approach, the following assumptions were taken into account: i) the luminescence quantum yield and the normalized emission spectrum of the fluorophore are independent of the excitation wavelength, ii) a fraction of the emitted photons are re-absorbed by the components of the sample and photons absorbed by the emitting species may lead to re-emission. The re-emitted photons may be further re-absorbed and so forth, iii) the system behaves as a homogeneous ideal scattering and absorbing material, iv) no radiation is transmitted through the sample, v) the sample is irradiated by monochromatic light, vi) emission is produced in each volume element and it is decomposed into two-photon flows having the same magnitude but opposite directions.

The correction derived from this approach leads to the following expression (Eq. (20)) for the quotient between the fluorescence ratio in a chloroplast and the fluorescence ratio in the TOC (FR_{chl}/FR_{TOC}):

$$\left(\frac{FR_{chl}}{FR_{TOC}}\right) = \frac{\chi_{(685)}/\gamma_{(685)}}{\chi_{(740)}/\gamma_{(740)}} = 3,86 \pm 0,14. \quad (20)$$

It is interesting to note the magnitude of this correction when drawing physiological conclusions from the fluorescence ratio. As shown here and in Fig. 6, a fluorescence ratio of 0.6 at canopy level implies a ratio of more or less 1 at leaf level and 2.3 at chloroplast level. It would be of great relevance to determine how fluorescence ratio changes between these three levels in different plant species and canopy structures.

7. Considerations and limitations for the model implementation in remote sensing

With regard to the application of the model in remote sensing, it is useful at this point to discuss the availability and/or accessibility of the inputs needed to calculate the correction factors $\chi(\lambda)$ and $\gamma(\lambda)$. Even more, it is interesting to think about the potential limitations that could arise.

To retrieve the spectral distribution of fluorescence at leaf level from that of the canopy, $\chi(\lambda)$ should be calculated and consequently R, Tc and Rb are required. The reflectance for the total system (R) is easily measured from the remote observation of the canopy.

With respect to canopy transmittance (Tc), even though it cannot be estimated from remote sensing measures, it can be reasonably calculated by a 1-D radiative transfer model as PROSAIL (Jacquemoud et al., 2009). In the case of an unidentified vegetable cover, parameters for a standard plant canopy can be used as input for the calculation of canopy transmittance (Jacquemoud et al., 2000). Moreover, if a known vegetable cover is being measured, more specific parameters can be entered in the model in order to simulate canopy transmittance. Furthermore, as our light re-absorption model shows low sensitivity to changes in canopy transmittance (as shown in Fig. 7), using transmittance spectra with moderate deviations from the real one, should not have great impact on the calculated correction factor.

Regarding the estimation of soil reflectance (Rb), two different alternatives may be available. Provided there is a portion of land free of plant cover, its reflectance may be remotely measured and used as input in the model, whenever this portion may be considered equivalent to that underneath the canopy. In the case this option is not available; a standard soil reflectance for this region can be used, since it has been shown here to have a low impact on fluorescence correction. The United States Geological Survey (USGS) spectral library (Kokaly et al., 2017) or the ASTER spectral library of the National Aeronautics and Space Administration (NASA) (Baldridge et al., 2009) may be useful in this case.

To reach the chloroplast level, it is additionally necessary to estimate the function $\gamma(\lambda)$ which in turn depends on the leaf level reflectance. When only measures at TOC are available, it would still be possible to apply the leaf-level correction using as an approximation reflectance spectra of leaves taken from spectral libraries such as LOPEX93 database (Hosgood et al., 1995) or ANGERS dataset (Féret et al., 2008). Another possible alternative would be to simulate the reflectance spectra of the leaves from radiative transfer models such as PROSPECT or PROSAIL. It should be noticed that, to apply the $\gamma(\lambda)$ correction function, strictly the reflectance of a thick layer of leaves must be known. When this value is not experimentally available, it is still possible to calculate the remission function to be used in Eq. (18) from reflectance and transmittance of a single leaf, using the pile of plates model (for details see Cordón and Lagorio, 2007).

Another important point to be discussed is the canopy architecture. Several recent works reported that chlorophyll fluorescence observed by remote sensing was affected by the canopy structure and viewing geometry (Liu et al., 2016; Migliavacca et al., 2017; Pinto et al., 2017; He et al., 2017). In the presented model (from leaf level to canopy) a homogeneous canopy was assumed. The species *F. benjamina*, used in this study, met these requirements and the model accurately predicted the spectral distribution of fluorescence at leaf level from that of the canopy. Lack of homogeneity in a canopy could however affect the applicability of the model.

Studies on different canopies to establish more precisely the goodness and universal applicability of the model are relevant for future work. These works should include variations in canopies architecture (planophile vs erectophile), differences in the amount of biomass or leaf area index and introduction of heterogeneity factors caused by the presence of flowers, fruits or senescent material, among others.

Finally, it is important to highlight that in this work, we present the correction model and its validation for excitation with monochromatic light. In its present form, the model is suitable for applications in remote sensing using LASER-induced chlorophyll fluorescence.

The model is extensible to polychromatic light by allowing variation of λ_0. Differences appear in the expression for the absorbed photon flux in Eq. (9), where an integral between the excitation wavelengths $\lambda_{0(1)}$ and $\lambda_{0(2)}$ should be introduced:

$$dI_F(\lambda) = \varphi_F \cdot g(\lambda) \cdot \int_{\lambda_{0(1)}}^{\lambda_{0(2)}} [I_x\{1 - \exp[-\alpha(\lambda_0)dx]\} + I_{xb}\{1 - \exp[-\alpha(\lambda_0)dx_b]\}]\, d\lambda_0.$$

Moreover, subsequent equations must be modified accordingly. Light polychromaticity requires future work for both the mathematical resolution and the validation process.

8. Conclusions and perspectives

In this work, we have developed a model of a generic canopy, taking into account the photon fluxes involved in the absorption, emission and re-absorption processes. Using this approach, the fluorescence spectra at TOC is corrected by a χ factor which is function of the reflectance and transmittance of canopy and soil reflectance. By measuring fluorescence spectra at both leaf level and canopy level, we have verified that our model accurately accounts for the re-absorption processes within the canopy and estimates the leaf spectral distribution from that of the canopy. Therefore, this model provides the missing link between fluorescence spectra measured at TOC and leaf fluorescence -which is the most known and studied level- and quantifies fluorescence re-absorption in the canopy, a phenomenon that has been mentioned but never quantified in literature.

Moreover, this model could retrieve fluorescence spectra at leaf or chloroplast level from a large scale plant cover, when measuring fluorescence at middle scales with active sensing techniques (Andersen et al., 2006; Goulas et al., 2014), thus overcoming leaf to leaf heterogeneity, which is a problem when trying to diagnose several plants (Cendrero-Mateo et al., 2016).

Furthermore, as it is possible to retrieve the spectral distribution of fluorescence of chloroplasts from that at leaf level by measuring leaf reflectance (Ramos and Lagorio, 2004), we were able to predict the shape of chloroplast spectrum, starting from that of the canopy. We have also shown how fluorescence ratio, an important tool in plant physiology, changes dramatically between canopy, leaf and chloroplasts due to light re-absorption processes. Thus, the new physical approach presented here contributes extensively to the knowledge of chlorophyll fluorescence and, more importantly, to the interpretation of the observed signals from a distance, allowing the retrieval of microscopic information from remote signals.

Acknowledgments

The authors are grateful to the University of Buenos Aires (UBACyT 20020130100166BA) and to the Agencia Nacional de Promoción Científica y Tecnológica (PICT 2012-2357) for the financial support. M.G.L. and G.B.C. are researcher scientists of CONICET. J.M.R. developed this work with a fellowship from CONICET (Argentina).

Appendix A. Supplementary data

Supplementary data to this article can be found online at https://doi.org/10.1016/j.rse.2017.10.035.

References

Agati, G., 1998. Response of the in vivo chlorophyll fluorescence spectrum to environmental factors and laser excitation wavelength. Pure Appl. Opt. 7 (4), 797. http://dx.doi.org/10.1088/0963-9659/7/4/016.

Agati, G., Fusi, F., Mazzinghi, P., 1993. A simple approach to evaluation of the re-absorption of chlorophyll fluorescence spectra in intact leaves. J. Photochem. Photobiol. B. 17, 163. http://dx.doi.org/10.1016/1011-1344(93)80009-X.
Andersen, H., Reutebuch, S.E., Mcgaughey, R.J., 2006. Active remote sensing. Comp. Appl. Sust. F. Man. 43–66.
Bah, T., 2009. Inkscape: Guide to a Vector Drawing Program (Digital Short Cut). Pearson Education ISBN-13: 978-0-13-276414-8.
Baldridge, A.M., Hook, S.J., Grove, C.I., Rivera, G., 2009. The ASTER spectral library version 2.0. Remote Sens. Environ. 113 (4), 711–715. http://dx.doi.org/10.1016/j.rse.2008.11.007.
Cendrero-Mateo, M.P., Moran, M.S., Papuga, S.A., Thorp, K.R., Alonso, L., Moreno, J., Ponce-Campos, G., Rascher, U., Wang, G., 2016. Plant chlorophyll fluorescence: active and passive measurements at canopy and leaf scales with different nitrogen treatments. J. Exp. Bot. 67 (1), 275–286. http://dx.doi.org/10.1093/jxb/erv456.
Cerovic, Z.G., Goulas, Y., Gorbunov, M., Briantais, J.M., Camenen, L., Moya, I., 1996. Fluorosensing of water stress in plants. Diurnal changes of the mean lifetime and yield of chlorophyll fluorescence measured simultaneously and at distance with a τ - LIDAR and a modified PAM-fluorimeter, in maize, sugar beet and Kalanchoë. Remote Sens. Environ. 58, 311–321. http://dx.doi.org/10.1016/S0034-4257(96)00076-4.
Cordon, G., Lagorio, M.G., 2006. Re-absorption of chlorophyll fluorescence in leaves revisited. A comparison of correction models. J. Photochem. Photobiol. Sci. 5, 735–740. http://dx.doi.org/10.1039/B517610G.
Cordón, G.B., Lagorio, M.G., 2007. Optical properties of the adaxial and abaxial faces of leaves. Chlorophyll fluorescence, absorption and scattering coefficients. Photochem. Photobiol. Sci. 6 (8), 873–882. http://dx.doi.org/10.1039/B617685B.
Damm, A., Elbers, J., Erler, A., Gioli, B., Hamdi, K., Hutjes, R., Kosvancova, M., Meroni, M., Miglietta, F., Moersch, A., Moreno, J., Schickling, R., Udelhoven, T., van der Linden, S., Hostert, P., Rascher, U., 2010. Remote sensing of sun induced fluorescence to improve modeling of diurnal courses of gross primary production (GPP). Glob. Chang. Biol. 16, 171–186. http://dx.doi.org/10.1111/j.1365-2486.2009.01908.x.
Daumard, F., Goulas, Y., Champagne, S., Fournier, A., Ounis, A., Olioso, A., Moya, I., 2012. Continuous monitoring of canopy level sun-induced chlorophyll fluorescence during the growth of a sorghum field. IEEE Trans. Geosci. Remote Sens. 50 (11), 4292–4300. http://dx.doi.org/10.1109/TGRS.2012.2193131.
Dawson, T.P., Curran, P.J., Plummer, S.E., 1998. LIBERTY - modeling the effects of leaf biochemical concentration on reflectance spectra. Remote Sens. Environ. 65 (1), 50–60. http://dx.doi.org/10.1016/S0034-4257(98)00007-8.
Féret, J.B., François, C., Asner, G.P., Gitelson, A.A., Martin, R.E., Bidel, L.P., Ustin, S.L., Maire le, Guerric, Jacquemoud, S., 2008. PROSPECT-4 and 5: advances in the leaf optical properties model separating photosynthetic pigments. Remote Sens. Environ. 112 (6), 3030–3043. http://dx.doi.org/10.1016/j.rse.2008.02.012.
Fournier, A., Daumard, F., Champagne, S., Ounis, A., Goulas, Y., Moya, I., 2012. Effect of canopy structure on sun-induced chlorophyll fluorescence. ISPRS J. Photogramm. Remote Sens. 68, 112–120. http://dx.doi.org/10.1016/j.isprsjprs.2012.01.003.
Franck, F., Juneau, P., Popovic, R., 2002. Resolution of the photosystem I and photosystem II contributions to chlorophyll fluorescence of intact leaves at room temperature. Biochim. Biophys. Acta 1556 (2), 239–246. http://dx.doi.org/10.1016/S0005-2728(02)00366-3.
Freedman, A., Cavender-Bares, J., Kebabian, P.L., Bhaskar, R., Scott, H., Bazzaz, F.A., 2002. Remote sensing of solar-excited plant fluorescence as a measure of photosynthetic rate. Photosynthetica 40, 127–132. http://dx.doi.org/10.1023/A:1020131332107.
Gastellu-Etchegorry, J.P., Grau, E., Lauret, N., 2012. In: Alexandru, Prof. Catalin (Ed.), DART: A 3D Model for Remote Sensing Images and Radiative Budget of Earth Surfaces in Modeling and Simulation in Engineering. InTech. http://dx.doi.org/10.5772/31315.
Gitelson, A., Buschmann, C., Lichtenthaler, H., 1998. Leaf chlorophyll fluorescence corrected for reabsorption by means of absorption and reflectance measurements. J. Plant Physiol. 152, 283. http://dx.doi.org/10.1016/S0176-1617(98)80143-0.
Goulas, Y., Ounis, A., Daumard, F., Baret, F., Chelle, M., Moya, I., 2014. Assessment of canopy fluorescence yield with airborne passive and active measurements: the Calsif Project. 5th Int. Work. Rem. Sens.Veg. Fluoresc. 1.
Grace, J., Nichol, C., Disney, M., Lewis, P., Quaife, T., Bowyer, P., 2007. Can we measure terrestrial photosynthesis from space directly, using spectral reflectance and fluorescence? Glob. Ch. Biol. 13 (7), 1484–1497. http://dx.doi.org/10.1111/j.1365-2486.2007.01352.x.
Guanter, L., Alonso, L., Gómez-Chova, L., Amorós-López, J., Vila, J., Moreno, J., 2007. Estimation of solar-induced vegetation fluorescence from space measurements. Geophys. Res. Lett. 34 (8). http://dx.doi.org/10.1029/2007GL029289.
Guanter, L., Zhang, Y., Jung, M., Joiner, J., Voigt, M., Berry, J.A., Frankenberg, C., Huetef, A.R., Zarco-Tejada, P.J., Lee, J.-E., Moran, M.S., Ponce-Campos, G., Beer, C., Camps-Valls, G., Buchmann, N., Gianelle, D., Klumpp, K., Cescatti, A., Baker, J.M., Griffis, T.J., 2014. Global and time-resolved monitoring of crop photosynthesis with chlorophyll fluorescence. Proc. Natl. Acad. Sci. U. S. A. 111 (14), E1327–E1333. http://dx.doi.org/10.1073/pnas.1320008111.
He, L., Chen, J.M., Liu, J., Mo, G., Joiner, J., 2017. Angular normalization of GOME-2 sun-induced chlorophyll fluorescence observation as a better proxy of vegetation productivity. Geophys. Res. Lett. 44 (11), 5691–5699. http://dx.doi.org/10.1002/2017GL073708.
Hosgood, B., Jacquemoud, S., Andreoli, G., Verdebout, J., Pedrini, G., Schmuck, G., 1995. Leaf optical Properties Experiment 93 (LOPEX93). Ispra, Italy. http://opticleaf.ipgp.fr.
Iriel, A., Mendes Novo, J., Cordon, G.B., Lagorio, M.G., 2014. Atrazine and methyl viologen effects on chlorophyll-a fluorescence revisited. Implications in photosystems emission and ecotoxicity. J. Photochem. Photobiol. 90, 107. http://dx.doi.org/10.1111/php.12142.
Jacquemoud, S., Baret, F., 1990. PROSPECT: a model of leaf optical properties spectra. Remote Sens. Environ. 34, 75–91.
Jacquemoud, S., Bacour, C., Poilve, H., Frangi, J.P., 2000. Comparison of four radiative transfer models to simulate plant canopies reflectance: direct and inverse mode. Remote Sens. Environ. 74 (3), 471–481. http://dx.doi.org/10.1016/S0034-4257(00)00139-5.
Jacquemoud, S., Verhoef, W., Baret, F., Bacour, C., Zarco-Tejada, P.L., Asner, G.P., François, C., Ustin, S.L., 2009. PROSPECT + SAIL models: a review of use for vegetation characterization. Remote Sens. Environ. 113, S56–S66. http://dx.doi.org/10.1016/j.rse.2008.01.026.
Joiner, J., Yoshida, Y., Vasilkov, A.P., Middleton, E.M., Campbell, P.K.E., Yoshida, Y., Kuze, A., Corp, L.A., 2012. Filling-in of near-infrared solar lines by terrestrial fluorescence and other geophysical effects: simulations and space-based observations from SCIAMACHY and GOSAT. Atmos. Meas. Tech. 5 (4), 809–829.
Julitta, T., Corp, L.A., Rossini, M., Burkart, A., Cogliati, S., Davies, N., Hom, M., Mac Arthur, A., Middleton, E.M., Rascher, U., Schickling, A., Colombo, R., 2016. Comparison of sun-induced chlorophyll fluorescence estimates obtained from four portable field spectroradiometer. Remote Sens. 8 (2), 122 (doi:10.3390/rs8020122).
Kokaly, R.F., Clark, R.N., Swayze, G.A., Livo, K.E., Hoefen, T.M., Pearson, N.C., Wise, R.A., Benzel, W.M., Lowers, H.A., Driscoll, R.L., Klein, A.J., 2017. USGS spectral library version 7. Us Geog. Surv. http://dx.doi.org/10.3133/ds1035.
Lagorio, M.G., Dicelio, L., Litter, M., San Román, E., 1998. Modeling of fluorescence quantum yields of supported dyes. Aluminum carboxyphthalocyanine on cellulose. J. Chem. Soc. Faraday Trans. 94, 419–425. http://dx.doi.org/10.1039/A706113G.
Lichtenthaler, H.K., Buschmann, C., Knapp, C., 2005. How to correctly determine the different chlorophyll fluorescence parameters and the chlorophyll fluorescence decrease ratio RFd of leaves with the PAM fluorometer. Photosynthetica 43 (3), 379–393. http://dx.doi.org/10.5194/amt-5-809-2012.
Ligot, G., Balandier, P., Courbaud, B., Claessens, H., 2014. Forest radiative transfer models: which approach for which application? Can. J. For. Res. 44 (5), 385–397. http://dx.doi.org/10.1139/cjfr-2013-0494.
Liu, L., Liu, X., Wang, Z., Zhang, B., 2016. Measurement and analysis of bidirectional SIF emissions in wheat canopies. IEEE Trans. Geosci. Rem. Sens. 54 (5), 2640–2651. http://dx.doi.org/10.1109/TGRS.2015.2504089.
Louis, J., Ounis, A., Ducruet, J.-M., Evain, S., Laurila, T., Thum, T., Aurela, M., Wingsle, G., Alonso, L., Pedros, R., Moya, I., 2005. Remote sensing of sunlight-induced chlorophyll fluorescence and reflectance of Scots pine in the boreal forest during spring recovery. Remote Sens. Environ. 96, 37–48. http://dx.doi.org/10.1016/j.rse.2005.01.013.
Maxwell, K., Johnson, G.N., 2000. Chlorophyll fluorescence — a practical guide. J. Exp. Bot. 51 (345), 659–668. http://dx.doi.org/10.1093/jexbot/51.345.659.
Mazzinghi, P., Agati, G., Fusi, F., 1994. In: Stein, T.I. (Ed.), Interpretation and Physiological Significance of Blue-green and Red Vegetation Fluorescence in International Geoscience and Remote Sensing Symposium (IGARSS) '94, pp. 640. http://dx.doi.org/10.1109/IGARSS.1994.399207. (Pasadena, CA).
Meroni, M., Colombo, R., 2006. Leaf level detection of solar induced chlorophyll fluorescence by means of a subnanometer resolution spectroradiometer. Remote Sens. Environ. 103, 438–448. http://dx.doi.org/10.1016/j.rse.2006.03.016.
Meroni, M., Rossini, M., Guanter, L., Alonso, L., Rascher, U., Colombo, R., Moreno, J., 2009. Remote sensing of solar-induced chlorophyll fluorescence: review of methods and applications. Remote Sens. Environ. 113, 2037–2051. http://dx.doi.org/10.1016/j.rse.2009.05.003.
Migliavacca, M., Perez-Priego, O., Rossini, M., El-Madany, T.S., Moreno, G., van der Tol, C., Rascher, U., Berninger, A., Bessenbacher, V., Burkart, A., Carrara, A., Fava, F., Guan, J.-H., Hammer, T.W., Henkel, K., Juarez-Alcalde, E., Julitta, T., Kolle, O., Martín, M.P., Musavi, T., Pacheco-Labrador, J., Pérez-Burgueño, A., Wutzler, T., Zaehle, S., Reichstein, M., 2017. Plant functional traits and canopy structure control the relationship between photosynthetic CO_2 uptake and far-red sun-induced fluorescence in a Mediterranean grassland under different nutrient availability. New Phytol. 214, 1078–1091. http://dx.doi.org/10.1111/nph.14437.
Moya, I., Cerovic, Z., 2004. In: Papageorgiou, G.C. (Ed.), Remote Sensing of Chlorophyll Fluorescence: Instrumentation and Analysis. Chlorophyll-a Fluorescence: A Signature of Photosynthesis. Springer, Dordrecht, The Netherlands, pp. 429–445 (doi:10.1007/978-1-4020-3218-9_16).
North, P.R.J., 1996. Three-dimensional forest light interaction model using a Monte Carlo method. IEEE Trans. Geosc. Rem. Sens. 34, 946–956. http://dx.doi.org/10.1109/36.508411.
Ounis, A., Bach, J., Mahjoub, A., Daumard, F., Moya, I., Goulas, Y., 2016. A new airborne LiDAR for remote sensing of canopy fluorescence and vertical profile. EPJ Web of Conferences 119, 25019. http://dx.doi.org/10.1051/epjconf/201611925019.
Pedrós, R., Goulas, Y., Jacquemoud, S., Louis, J., Moya, I., 2010. FluorMODleaf: a new leaf fluorescence emission model based on the PROSPECT model. Remote Sens. Environ. 114, 155–167. http://dx.doi.org/10.1016/j.rse.2009.08.019.
Pfündel, E., 1998. Estimating the contribution of photosystem I to total leaf chlorophyll fluorescence. Photosynth. Res. 56, 185 (doi:10.1023/A:1006032804606).
Pinto, F., Müller-Linow, M., Schickling, A., Cendrero-Mateo, M.P., Ballvora, A., Rascher, U., 2017. Multiangular observation of canopy sun-induced chlorophyll fluorescence by combining imaging spectroscopy and stereoscopy. Remote Sens. 9, 415. http://dx.doi.org/10.3390/rs9050415.
Porcar-Castell, A., Tyystjärvi, E., Atherton, J., van der Tol, C., Flexas, J., Pfündel, E.E., Erhard, E., Moreno, J., Frankenberg, C., Berry, J.A., 2014. Linking chlorophyll a fluorescence to photosynthesis for remote sensing applications: mechanisms and challenges. J. Exp. Bot. doi:https://doi.org/10.1093/jxb/eru191 (eru191).
Ramos, M.E., Lagorio, M.G., 2004. True fluorescence spectra of leaves. J. Photochem. Photobiol. Sci. 3, 1063 (doi:10.1039/B406525E).
Ramos, M.E., Lagorio, M.G., 2006. A model considering light reabsorption processes to

correct *in vivo* chlorophyll fluorescence spectra in apples. Photochem. Photobiol. Sci. 5, 508–512. http://dx.doi.org/10.1039/B514248B.

Rascher, U., et al., 2009. CEFLES2: the remote sensing component to quantify photosynthetic efficiency from the leaf to the region by measuring sun-induced fluorescence in the oxygen absorption bands. Biogeosci. Discuss. 6 (1).

Rienzo Di, J.A., Casanoves, F., Balzarini, M.G., Gonzalez, L., Tablada, M., Robledo, Y.C., 2011. InfoStat Versión 2011. Grupo InfoStat, FCA. 8. Universidad Nacional de Córdoba, Argentina, pp. 195–199.

Rossini, M., Meroni, M., Celesti, M., Cogliati, S., Julitta, T., Panigada, C., Rascher, U., van der Tol, C., Colombo, R., 2016. Analysis of red and far-red sun-induced chlorophyll fluorescence and their ratio in different canopies based on observed and modeled data. Remote Sens. 8 (5), 412. http://dx.doi.org/10.3390/rs8050412.

Stuckens, J., Verstraeten, W.W., Delalieux, S., Swennen, R., Coppin, P., 2009. A dorsiventral leaf radiative transfer model: development, validation and improved model inversion techniques. Remote Sens. Environ. 113, 2560–2573. http://dx.doi.org/10.1016/j.rse.2009.07.014.

Vilfan, N., van der Tol, C., Muller, O., Rascher, U., Verhoef, W., 2016. Fluspect-B: a model for leaf fluorescence, reflectance and transmittance spectra. Remote Sens. Environ. 186, 596–615. http://dx.doi.org/10.1016/j.rse.2016.09.017.

van der Walt, S., Colbert, S.C., Varoquaux, G., 2011. The NumPy array: a structure for efficient numerical computation. Comput. Sci. Eng. 13 (2), 22–30. http://dx.doi.org/10.1109/MCSE.2011.37.

Wittenberghe van, S., Alonso, L., Verrelst, J., Hermans, I., Valcke, R., Veroustraete, F., Moreno, J., Samson, R., 2014. A field study on solar-induced chlorophyll fluorescence and pigment parameters along a vertical canopy gradient of four tree species in an urban environment. Sci. Total Environ. 466, 185–194. http://dx.doi.org/10.1016/j.scitotenv.2013.07.024.

Zelle, J.M., 2004. Python Programming: An Introduction to Computer Science. Franklin, Beedle Associates Inc.

Zhao, F., Dai, X., Verhoef, W., Guo, Y., van der Tol, C., Li, Y., Huang, Y., 2016. FluorWPS: a Monte Carlo ray-tracing model to compute sun-induced chlorophyll fluorescence of three-dimensional canopy. Remote Sens. Environ. 187, 385–399. http://dx.doi.org/10.1016/j.rse.2016.10.036.